NASA Contractor Report 198314

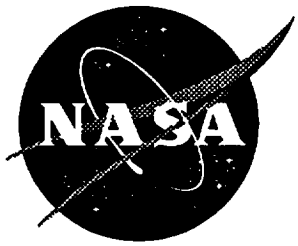

Multipath Analysis Diffraction Calculations

Richard B. Statham
Lockheed Martin Engineering & Sciences Company
Hampton, Virginia

Contract NAS1-19000

May 1996

National Aeronautics and
Space Administration
Langley Research Center
Hampton, Virginia 23681-0001

Multipath Analysis
Diffraction Calculations

Abstract

This report describes extensions of the Kirchhoff diffraction equation to higher edge terms and discusses their suitability to model diffraction multipath effects of a small satellite structure. When receiving signals, at a satellite, from the Global Positioning System (GPS), reflected signals from the satellite structure result in multipath errors in the determination of the satellite position. Multipath error can be caused by diffraction of the reflected signals and a method of calculating this diffraction is required when using a facet model of the satellite. Several aspects of the Kirchhoff equation are discussed and numerical examples, in the near and far fields, are shown. The vector form of the extended Kirchhoff equation, by adding the Larmor-Tedone and Kottler edge terms, is given as a Mathematica model in an appendix. The Kirchhoff equation was investigated as being easily implemented and of good accuracy in the basic form, especially in phase determination. The basic Kirchhoff can be extended for higher accuracy if desired. A brief discussion of the method of moments and the geometric theory of diffraction is included, but seem to offer no clear advantage in implementation over the Kirchhoff for facet models.

This work was performed by Lockheed Martin Engineering & Sciences, Langley Program Office under contract NAS1 - 19000 as part of Work Order CB002 under the direction of Dr. Steve J. Katzberg of the Space Systems and Concepts Division at the NASA Langley Research Center. The author would like to thank Dr. Katzberg for his support.

Table of Contents

List of Figures

Multipath Analysis
Diffraction Calculations

1.0 Introduction

The use of Global Positioning System (GPS) as a method of achieving satellite orientation and accurate orbit position of NASA mission satellites has been evaluated and has significant utility. One problem with this use is the reflection of microwaves from nearby satellite parts and the location of antennas on small satellites. These reflections (Figure 1) cause multiple paths from the GPS to the antenna and results in degraded positional information. This report describes methods of calculating the diffracted signal by use of the Fresnel-Kirchhoff (F-K) equation plus edge effects which are suitable for both the near (Fresnel) and far (Fraunhofer) field diffraction patterns for any flat plate. Work continues on evaluating other diffraction calculation methods.

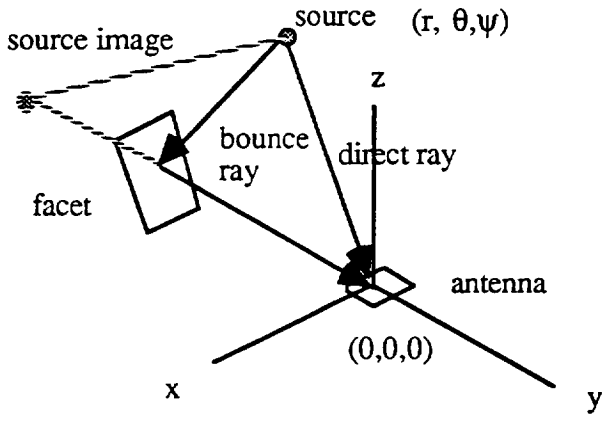

Figure 1 Geometry of Vector Facet Calculation

The approach used is to model a small satellite into facets and then to calculate the diffraction of each facet by means of the F-K equation. This is a relatively fast and straightforward way of calculating the multipath into the GPS receiver antenna. The accuracy of the F-K equations is good and a review of the 'edge effects' and the mathematical inconsistency of the F-K equation are discussed below. The technique should be sufficiently accurate in amplitude and phase from each facet to allow coherent summing of complex shapes. The greatest error will occur in curved surfaces in that the facet is a sample of the surface. If the facets are small enough, then the accuracy should be sufficient. A saving grace of the

technique, if it can be thought of as that, is that the F-K equation by itself is very good over the main lobe of the diffraction. It is also fairly accurate[1] out to 20-40 degrees off of the axis of specular reflection even for a small aperture ($\approx \lambda$ diameter) and close to the reflecting surface ($\leq \lambda$). It is felt that if the diffracted reflected ray is much less than the GPS direct ray, say 10% or so, then the amplitude and phase of the reflected ray will introduce negligible error into the heterodyned resultant signal used by the GPS receiver. Since the diffraction is basically a sinc function, then the main lobe of the reflected ray is of the most practical concern especially if the facets are small. The 'expanded' F-K equation, achieved by adding the Larmor-Tedone and the Kottler terms to the usual F-K equation, is even more accurate in the higher sidelobes.

There is a widely used method that gives an exact answer. This is the method of moments (MOM) or in an older terminology, the current distribution technique[2]. In this method, a series of sample points, or nodes, is excited by the incoming radiation, the surface current equilibrium solved and the re-radiated E field calculated. This method is very general and seems to be a method fully responsive to a general 3D metallic or semiconducting body with both light and dark areas. The method is simple but has a major problem. Extensive calculating resources are needed if the object is larger than several wavelengths. As an example[3], to correctly 'converge' the current amplitude distribution of a 0.47 λ long dipole, 60 nodes are required, giving a $\lambda/127$ sample spacing. This is in agreement with several other papers and is much more stringent than the $\lambda/5$ often quoted. No calculations have been done, to date, as to accuracy and speed using the MOM methods. Newer algorithms may mitigate this and the MOM approach or a variation of it should be investigated in the future.

Finally there are the Geometric Theory of Diffraction [4] (GTD) and the Physical Theory of Diffraction (PTD) methods. Both methods use, with different starting points, the idea that the total diffracted field, F_t can be split into a geometric ray part, F_{go} , and a diffraction ray, F_{diff}, giving $F_t = F_{go} + F_{diff}$. This approach has been developed into a highly usable technique in which an object or an edge diffraction is between the source and the observation point. The 'creeping wave' can be calculated and the resultant intensity of the diffraction calculated. The present approach has not yet addressed this problem, but it should be noted, that if the source is hidden behind an object, there is no direct ray to combine with the reflected ray at the antenna. Since the GTD/PTD methods are deeply grounded in the Rayleigh-Sommerfeld equations and are basically far field high frequency methods, they seem less attractive than the F-K method selected to date.

A final remark is <u>all mathematical or physical models that accurately predict the real world behavior are equal</u>. Various experiments (Andrews 1947, Silver[5] 1962, Totzeck 1991) indicate that the F-K approach agrees very well with actual experimental measurements under varying conditions.

2.0 The Fresnel-Kirchhoff Equation

The Kirchhoff equation is usually given as[6];

$$\hat{\mathbf{U}}(x_p, y_p, z_p) = \frac{1}{4\Pi}\iint_{\Sigma} U \frac{\partial}{\partial r}\left(\frac{e^{-ikr}}{r}\right)\{\hat{\mathbf{r}} \bullet \hat{\mathbf{n}}\} - \{\left(\frac{e^{-ikr}}{r}\right)\hat{\nabla}U \bullet \hat{\mathbf{n}}\}d\Sigma \qquad \text{Eq 1}$$

where the input U is a spherical wave at p, the source point, as defined in Figure 2 with a vector amplitude $\hat{\mathbf{A}}$.

$$\mathbf{U} = \frac{\hat{\mathbf{A}}}{p} e^{-ikp}\hat{\mathbf{p}}$$

Given the usual assumptions that $p \approx p_o$ and $r \approx r_o$, then the above equation simplifies to the form usually seen[7] (Equation 2) where β is the angle between the vectors $\hat{\mathbf{p}}$ and $\hat{\mathbf{n}}$ and α is between $\hat{\mathbf{r}}$ and $\hat{\mathbf{n}}$.

$$\hat{\mathbf{U}}(x_p, y_p, z_p) = -\frac{i\hat{A}}{2\lambda}\iint_{\Sigma} \left(\frac{e^{-ik(r+p)}}{rp}\right)(\cos\beta - \cos\alpha)d\Sigma \qquad \text{Eq 2}$$

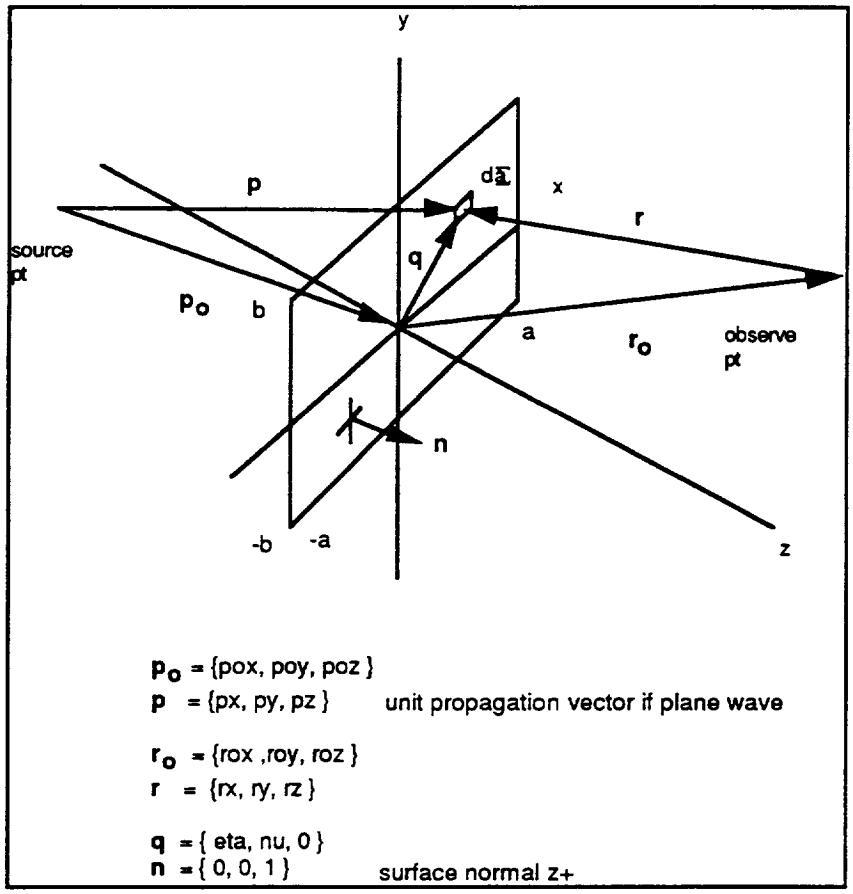

Figure 2 Definitions of Coordinates and Vectors Used

The mathematical inconsistency often discussed about the F-K equation concerns the interpretation of Equation 1. If $\partial U/\partial n = 0$ and $U=0$, which is a Kirchhoff assumption[8] beyond the aperture boundary, then the field U can be shown to be zero at any point. However another interpretation is possible. The first term in Equation 2 is the Rayleigh-Sommerfeld I term and is a solution to the Helmholtz equation. The second term is the Rayleigh-Sommerfeld II term and also is a solution to the Helmholtz equation. Both are mathematically consistent in the sense given above. Surprisingly, the R-S I, R-S II and F-K solutions give much the same answer in calculations of the resultant fields (see Totzeck 1991). The F-K equation is just the average of the R-S terms. In a similar manner, Babinet's principle has been questioned as to it validity but experimental results seem to agree very well with its conclusions.[9]

Equation 2 has been extensively used in the small angle approximation and far field calculations with much success. An improvement is to remove the small angle requirements and to carry the $r \neq r_o$, $p \neq p_o$ conditions. For a spherical wave input, the result is Equation 3 . It should be noted that $\hat{\mathbf{p}}$ and $\hat{\mathbf{r}}$ are not unit vectors but $\hat{\mathbf{n}}$ is a unit vector. It should also be

noted that $\hat{\mathbf{A}}$ or the field amplitude is a vector to allow polarization effects to be calculated.

$$\hat{\mathbf{U}}(x_p, y_p, z_p) = \frac{\hat{\mathbf{A}}}{4\Pi} \iint_{\Sigma} \frac{e^{-ik(p+r)}}{rp} [(ik + \frac{1}{p})\{\frac{\hat{\mathbf{p}}}{p} \bullet \hat{\mathbf{n}}\} - (ik + \frac{1}{r})\{\frac{\hat{\mathbf{r}}}{r} \bullet \hat{\mathbf{n}}\}] d\Sigma \quad \text{Eq 3}$$

The efforts on multipath delivered to date (Multipath Analysis, Diffraction Calculations, Interim Report #3, R Statham, Lockheed Engineering & Sciences, Nov. 1995) are based on Equation 2 where U is the E field component. The method can easily be extended by the use of Equation 3.

2.1 The Extended Fresnel-Kirchhoff Equation

The results of the equations above are the F-K equation as commonly stated. It is an integration over the aperture surface Σ and, as stated before, is accurate over a large range of conditions. There is much discussion in the literature of edge effects in diffraction and some clarification seems useful. The first point to be noted is that Equation 3 can be transformed[10] into a closed line integral by the use of Stoke's theorem. The first concern is to separate these two forms when edge effects are discussed. There are fundamental edge effects, however, adding to the basic F-K area integral. These were formulated by Kottler [11], who is stated to be the first to correctly develop the Huygens principle mathematically. The development shown below is after Karczewski.

Two terms must be added to the basic F-K equation to extend the F-K equation. The Larmor-Tedone term is an edge function similar to the edge function described by the geometric theory of diffraction. It is a 'donut' around the edge with a sinc cross section profile. The edge essentially acts as a line antenna. The third term to be added is the Kottler term, which is a cross term equation. While the effects of these higher terms will vary with specific boundary and scale values, they are normally much less that the F-K, or base term, which dominates in most cases. As an example, given a one meter square aperture and 0.19 cm wavelength plane wave, at 20 meters, the peak E field amplitude of the F-K term is 0.262, the Larmor-Tedone term is 0.00788 and the third or Kottler term is also 0.00788. Since the energy is the square of these values, it can be seen that the higher terms are essentially negligible in this case. The propagation vector direction of these terms also is of interest. The E-field of the F-K term, is in the same direction as the input (x axis), but the E-field of the second and third terms are along the z axis hence the propagation vector is in the xy plane. This can be seen in the second term for a symmetrical square aperture. Given four E-field 'edge donuts' in the x-y plane equally spaced from the z-axis, they would on-axis cancel except in the z direction. This is one reason the F-K term agrees so well near the on-axis conditions since an xy antenna would not register the z component. Off-axis has incomplete cancellation and an 'error' starts to appear. This is the genesis of statements such as '5 % diffraction error at the higher sidelobes ' or

'essential agreement'. The latter, measured in db, is used in the microwave area.

Another observation is that the F-K term is an area integral (surface Σ) with the higher terms being line integrals (edge(s) Γ). As the aperture gets smaller, the higher terms become more important since they decrease linearly and the F-K term decreases by the second power. A combination of a small aperture and off-axis conditions would cause the greatest divergence from the F-K term alone.

The 'expanded F-K' terms, for a plane wave input, are as follows;

$$\mathbf{Eo} = e^{-ik(\hat{r}\bullet\hat{p})} \qquad \text{input plane wave}$$

$$\mathbf{dipole} = \frac{e^{-ikr}}{r} \qquad \text{dipole function}$$

$$\hat{E}(x_p, y_p, z_p) = \frac{\hat{A}}{4\Pi}\iint_{\Sigma}\{Eo\frac{\partial(dipole)}{\partial r}\frac{\hat{r}}{r}\bullet\hat{n} - dipole\frac{\partial(Eo)}{\partial\hat{n}}\}d\Sigma \quad \text{First F-K term}$$

$$+\frac{1}{4\Pi}\oint_{\Gamma}[d\hat{s}\times\hat{A}\frac{e^{-ik(\hat{q}\bullet\hat{p}+r)}}{r}]d\Gamma \qquad \text{Second Larmor-Tedone term}$$

$$+\frac{1}{ik4\Pi}\oint_{\Gamma}[Eo\{d\hat{s}\bullet(\hat{p}\times\hat{A})\}grad_p(dipole)]d\Gamma \quad \text{Third Kottler term}$$

The equations are listed in Appendix B as a Mathematica program.

2.2 Example Results at 20 meters

Using a 1 x 1 meter square aperture with a wavelength of 0.19 m and a linear polarization in the x direction, the first or F-K term for an input normal to the aperture is shown below in Figure 3a. The image plane is 20 meters from the aperture and the x & y are $\pm$ 10 meters giving a 53 degree subtense. The peak amplitude is 0.262 normalized for a plane wave amplitude of 1.0 at the aperture. The first term vector is along the x axis only and is the E field vector {0.256-i 0.0575, 0, 0} at the axis. The phase was also plotted but is the usual 'semi-chaotic' plot, which provides little insight.

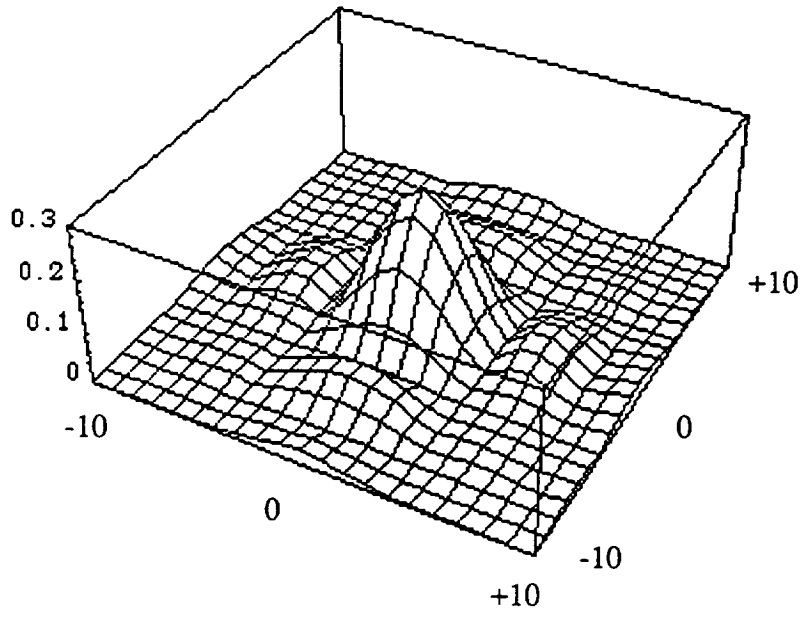

Figure 3a Amplitude of E field for the First or F-K Term
1 x 1 m aperture @ 20 m, λ = .19 m

The second term, the Larmor-Tedone term, is shown under the same conditions in Figure 3b. Note that the amplitude scale is much reduced as compared to the F-K term. The maximum amplitude is .00788 as stated before but is zero on axis. The second term effect is in the y direction only, due to the x polarized input. However, the full vector form of the second term is {0, 0, ((ay*dx - ax*dy)*E^(-I*k*(r + qvec . pvec)))/r}. From this, it can be seen that the integration is along the dy only since the input polarization is ax=1, ay=0 and az=0. in this example. It is also interesting that the output E field polarization is in the z axis direction. Since the Poynting vector is orthogonal to the E field vector, then the energy of the second term is propagated in the xy plane and is an evanescent wave component in the 'reactive zone' near the aperture. This agrees with Silver[12]. This gives insight to the corrections required by the F-K term at higher sidelobes where the small angle F-K equation approximation increasingly fails. Again, the total phase plot is chaotic and not very instructive visually. The phase of one edge only is shown in the +z domain , along with a one edge amplitude at 20 and 2 meters, in Figure 4.

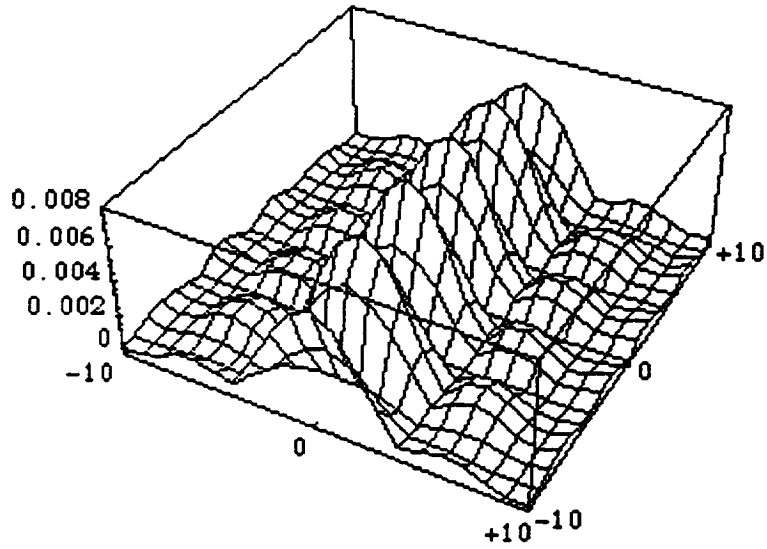

Figure 3b Amplitude of E field for the Second or L-T Term
1 x 1 m aperture @ 20 m, λ = .19 m

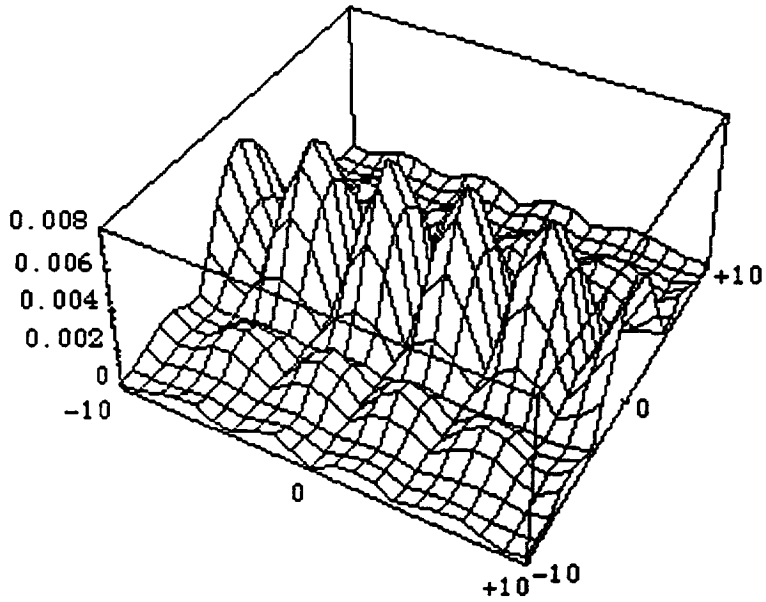

Figure 3c Amplitude of E field for the Third or Kottler Term
1 x 1 m aperture @ 20 m , λ = .19 m

The third, or Kottler term, is shown in Figure 3c. It is very similar to the L-T term in that it propagates, for x polarization and z propagation input, in the xy plane and is also part of the evanescent wave concept. The full vector, for this example, is {0, 0, -Φ[E^(eta,nu,pvec)] pz(dy(-(az*px) + ax*pz) + dx(az*py - ay*pz))(-I + k((eta - rox)^2 + (nu - roy)^2 + roz^2) ^(1/2))/(4kPi((eta - rox)^2 + (nu - roy)^2 + roz^2))}. In general, there are many cross terms between the amplitude and propagation vectors and the direction of integration of the edge

(dx,dy). Therefore, the third term can propagate in any x,y,+z direction depending on the specific polarization and input angles but in this specific example, the propagation is in the xy plane also. Again, the third term phase is chaotic and not very informative visually.

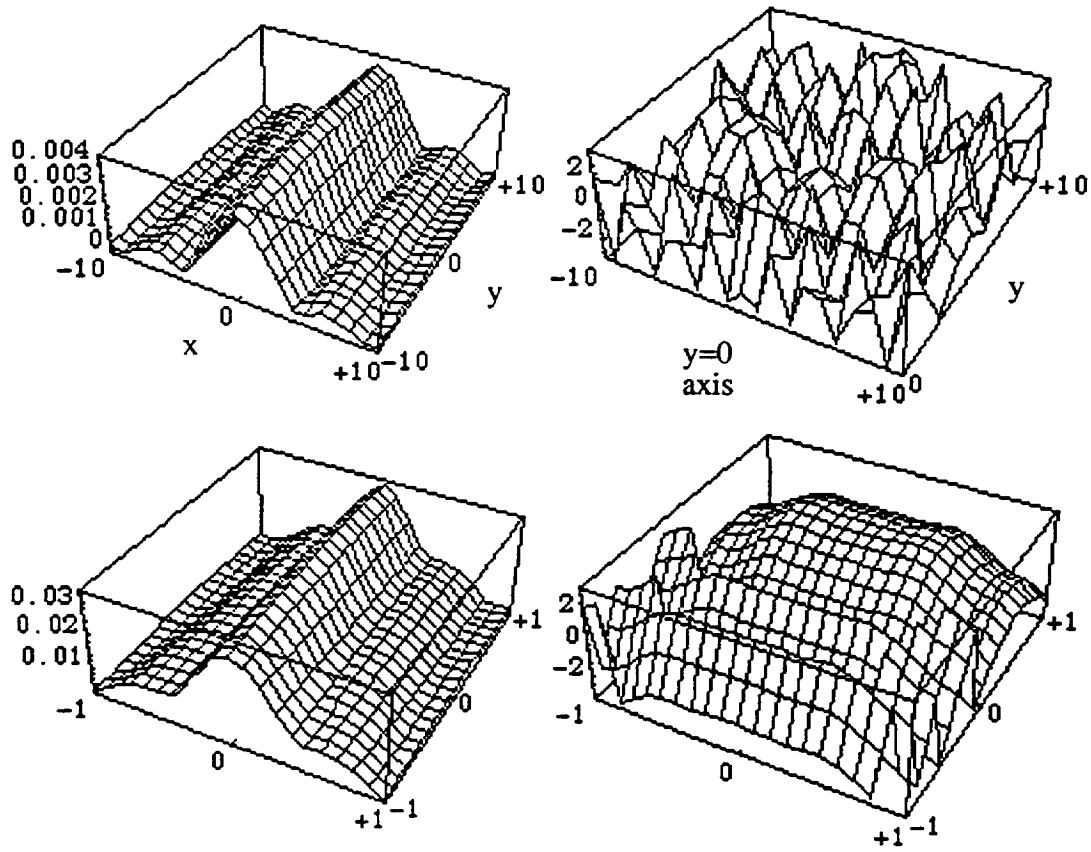

Figure 4 Amplitude & Phase of One Edge for the Second or L-T Term
1 x 1 m aperture @ 20 (top) & 2 (bottom) m , λ = .19 m

2.3 Example Results at 2 meters

The above results are more typical of a far field example since the image plane is at 20 meters. In Figure 5 a more typical near term example, a 1 x 1 m aperture, is shown, which is included as being more interesting both in amplitude and in phase. The image plane here is at 2 meters. All three terms are shown. The peak amplitudes are 1.764, 0.0638 and 0.0638 for the three terms. In this case, there appears to be structure in the phase figures, but one must be cautious since the sampling of the diagram is coarse (0.1 meters) at a 2 meter distance and a smaller sample interval is needed. Appendix A shows the effects of smaller apertures, from 0.19 to 0.6 meters square.

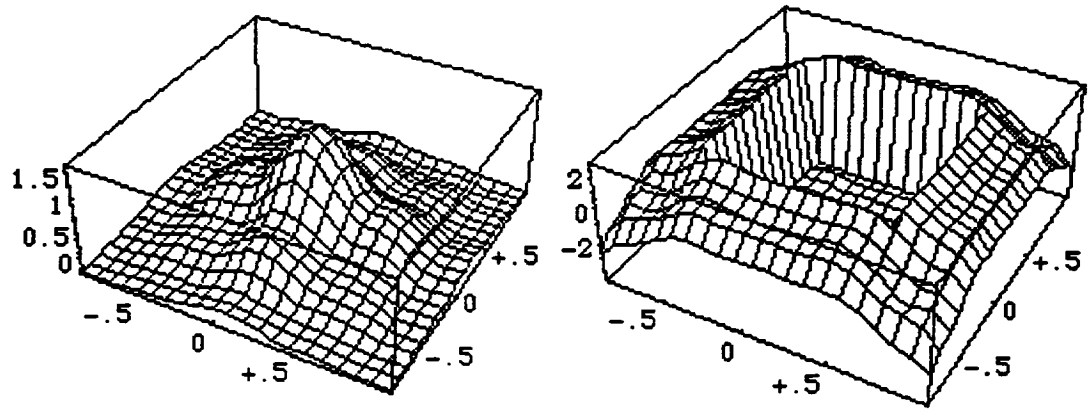

The First or F-K term

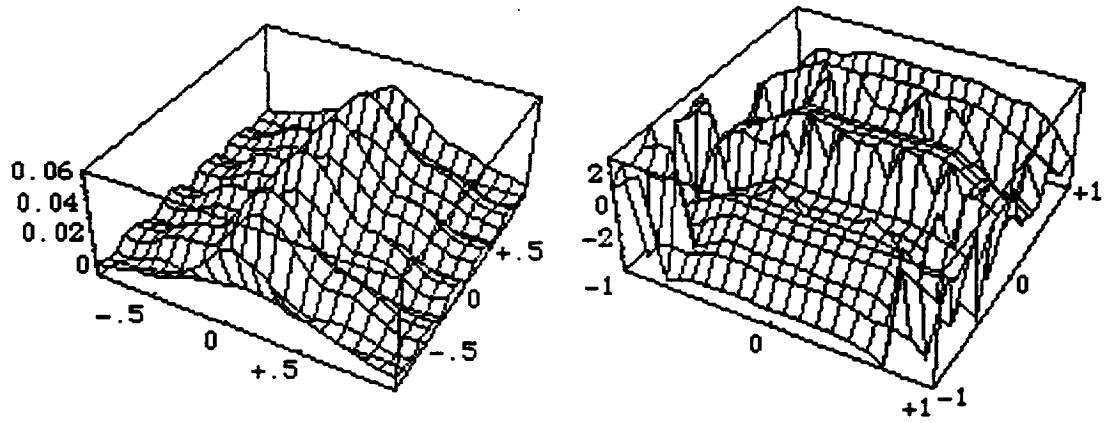

The Second or L-T term

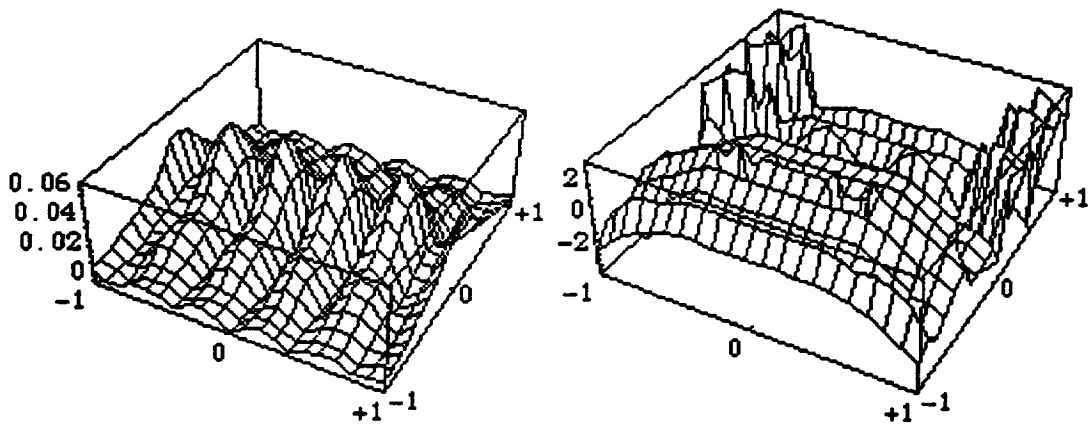

The Third or Kottler Term

Figure 5 Amplitude & Phase of Near Field Aperture
1 x 1 m aperture @ 2 m on-axis, λ = .19 m, x polarization

3.0 The Maggi Transform

As discussed earlier, the Fresnel-Kirchhoff equation can be put into a line integral form. This was done by Maggi[13] in 1888 and is the basis for much of the discussion of 'edge' effects but are due to the F-K term concepts. Actually Keller, in developing his GTD approach, used the Maggi transform with the Rubinowicz[14] evaluation for short wavelengths. It is important to keep track of the assumptions and arguments when evaluating the various diffraction methods and effects discussed. For a plane wave the Maggi transform[15] is;

$$\iint_S \left\{ \frac{e^{ikr}}{r} \frac{\partial}{\partial n} e^{ik\hat{r}_o \cdot \hat{p}} - e^{ik\hat{r}_o \cdot \hat{p}} \frac{\partial}{\partial n}\left(\frac{e^{ikr}}{r} \right) \right\} ds = -4\pi\varepsilon e^{ik\hat{r}_o \cdot \hat{p}} + \int_\Gamma \frac{e^{ik(\hat{r}_o \cdot \hat{p} + r)}}{r} \frac{\{\hat{p} \times \hat{r}\} \cdot \hat{t}}{r + \hat{p} \cdot \hat{r}} dt \qquad \text{Eq 4}$$

where $\hat{t}$ is the tangent vector at the edge. The interesting factor is ε, which is zero if a line from the source to the point of observation is hidden by the plane containing the aperture (in the shadow region) and is one if the observation point lies in the geometric 'bright' region of the aperture image. The term containing ε is just the geometric ray wave value. The second Maggi term is then just the 'diffraction ray' value, which is added to the 'geometric ray' value when appropriate. This is the genesis of partitioning the diffraction problem into geometric and diffraction components and is equal to the Kirchhoff equation.

4.0 Conclusions

The Kirchhoff equation has been the main approach to diffraction for a long time. It has also been under attack by new concepts and methods, especially after the 1970's. Many claims have been made of newer methods but most seem traceable to Huygen's principle, either as a radiating edge or as an area integration. One view is that Huygen 'secondary radiations' are not electromagnetic waves until they are summed in the final result , but inherently they must be summed over a closed surface. If the surface is not closed, then certain effects did not cancel exactly and error resulted. Kottler examined this and calculated the edge currents of incremental (da) radiators and carried the results into an additional term required to extend the Kirchhoff approach. To do so, he proposed a 'saltus' solution not a boundary one. A saltus problem provides solutions that satisfy the wave equation in the entire z+ space, not just at the boundary. The solution also satisfies "certain stepwise" discontinuities at the plane z=0 [Silver 1962]. This seems a reasonable approach since the edge, if real, certainly introduces

discontinuities. All approaches use at least one 'volume' limitation since they all assume that the radiation energy law is obeyed at infinity. Even though diffraction occurs at the edge, and has been much studied [Sommerfeld, Bouwkamp[16]], a saltus approach seems reasonable. As mentioned above, the Kirchhoff equation can also be considered to be the average solution of the mathematically consistent Rayleigh - Sommerfeld Type I and Type II solutions. These views are adopted here.

One of the great problems of diffraction, or even light itself, is how to partition the problem conceptually. The Kirchhoff equation is scalar but can be applied to each component of the polarized vector and can be cast into a vector form. Even more interesting is that the area equation can, by means of the Maggi transform, be considered a line or edge effect. If this is done then a 'geometric' term is left over and this has been the basis of much short wavelength 'ray' work, such as the Geometric Theory of Diffraction. The partitioning of the problem into the sum of geometric and diffraction 'rays' has been successful and development in this area continues with the UTD or Universal Theory of Diffraction. However, one must be careful of the assumptions built into each approach and use them only in their domain of applicability. The approach of the extended Kirchhoff concept seems to have the widest application under the broadest conditions.

A brief remark about the MOM or Method of Moments approach to diffraction seems in order. The MOM approach is conceptually satisfying but, as pointed out above, somewhat mathematically demanding in computer resources. It should be pointed out that the Kirchhoff equations are similar in that the equation is the integrated product of the input wave function and amplitude that modify the dipole function or $\Sigma[\Im$ [input wave (amplitude) function] $*\Im$ [dipole function]]. If both methods reasonably model actual experimental results, then they are approximately equal to each other. They do differ in implementation and may be selected due to specific conditions of a desired problem definition or the resources available.

The implementation of the diffraction calculation has been a major concern of this investigation. The problem defined in the first paragraphs, the multiple path reflection of the GPS signal off of small satellite surfaces, requires a general approach. It also requires a high degree of precision in the phase calculation since interference of wave forms is a major parameter to be calculated. The GPS carrier wave interference (direct vs. reflected) determines the signal amplitude and the modulated wave form phase, when heterodyned down, determines the measured positional accuracy of the system. The approach used is to model the small satellite into 'facets' and to calculate the contribution of the summed facets upon each measurement. Fairly simple facet models are contemplated. A model to calculate the specular and diffracted reflected ray from each facet, given the facet vertex coordinates, has been developed in prior efforts reported during this effort. The diffraction equation used was the scalar Fresnel - Kirchhoff cosine form (Eq 2) found in many references. This may be sufficient. If a more exact result is desired, then the vector F-K equation shown here can be easily updated into the software. If an extended F-K approach is needed (the 2nd and 3rd terms are relativity small however), then an all line integration is

suggested. That requires a geometric ray or 'light/shadow' determination, which will have to be implemented. This can be done in a straightforward manner.

The development was done on Mathematica Version 2.102 Enhanced using a Macintosh Centris 650. The calculations were done to 3 significant figures but periodically checked to 6 significant figures for accuracy. Three figures seemed sufficient for this overview but higher accuracy is desirable for GPS activities. The integrations were done using a Gauss-Kronrod integration algorithm with six recursive levels and four singularity levels which is the standard default. Run time was about one minute per value under the above conditions.

Appendix A

Diffraction Terms for Various Aperture Sizes at 2 meters

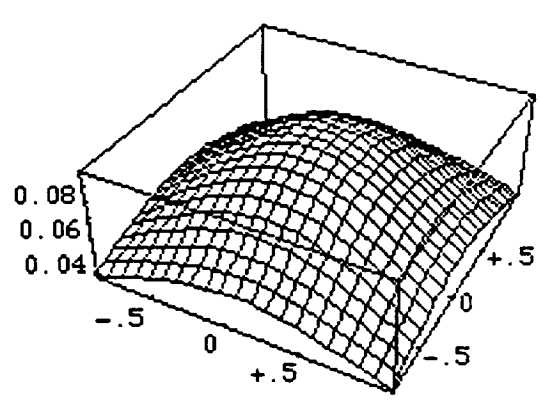

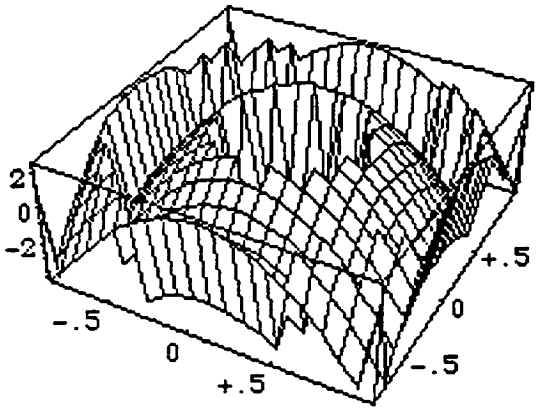

0.19 x0.19 m aperture max amp =0.0948 phase

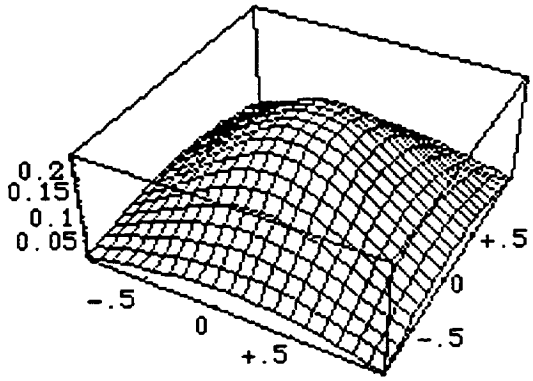

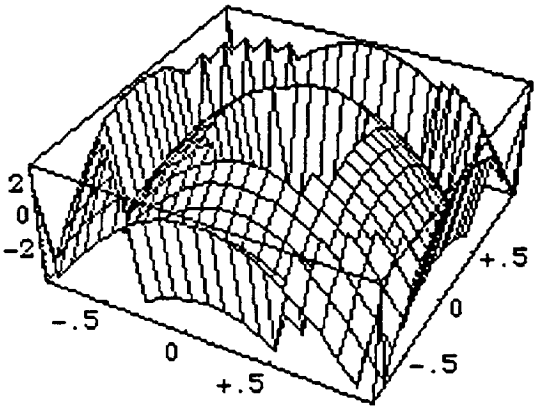

0.3 x 0.3 m aperture max amp =0.235 phase

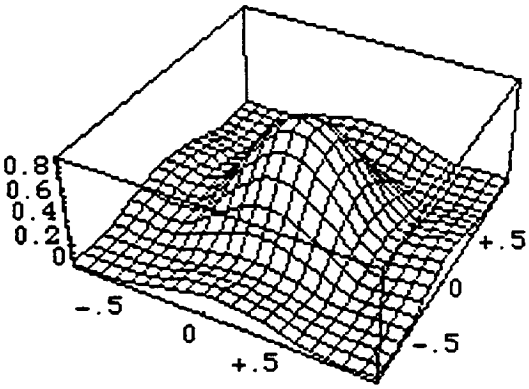

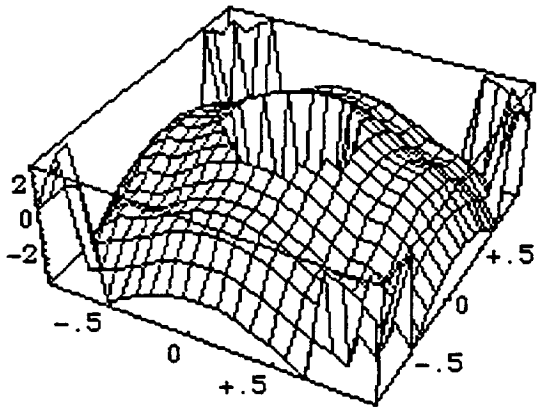

0.6 x 0.6 m aperture max amp =0.893 phase

Figure 6a Amplitude & Phase F-K Term for plane wave
(@ 2 meters, λ =.19 m)

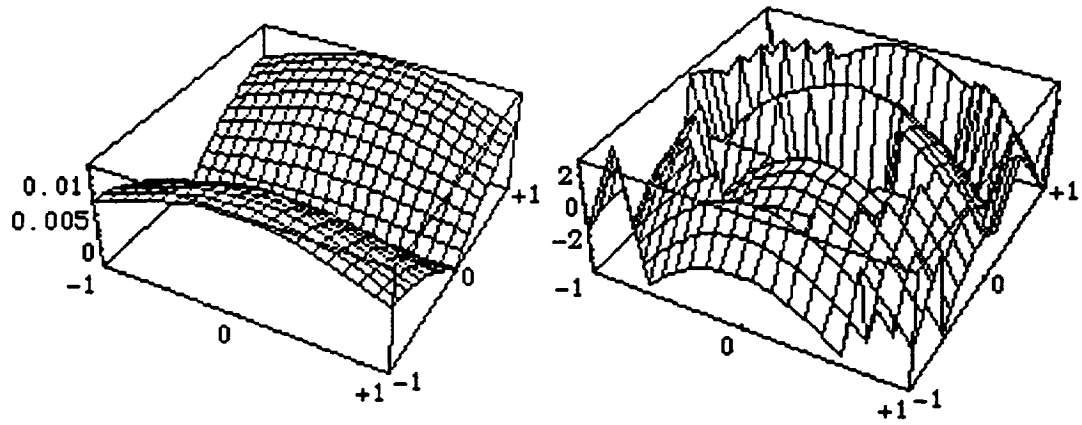

0.19 x 0.19 m aperture Max amp= 0.0133 phase

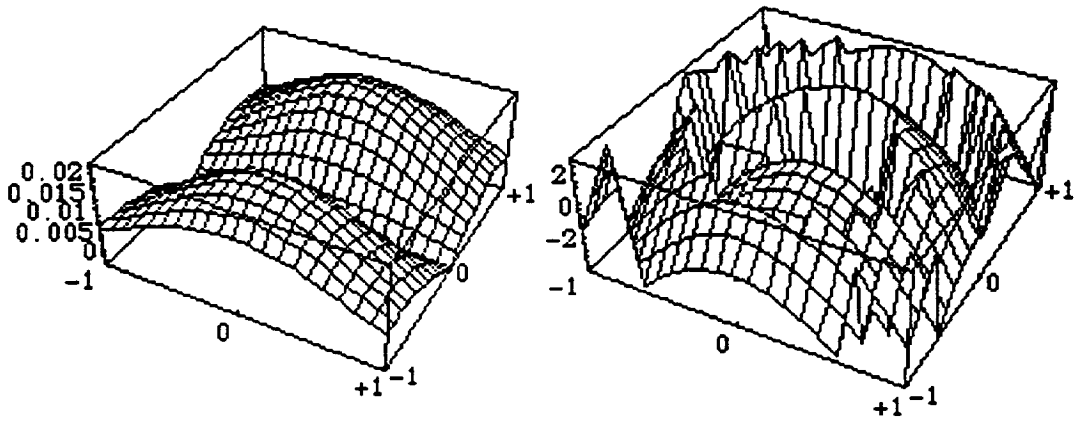

0.3 x 0.3 m aperture Max amp= 0.0225 phase

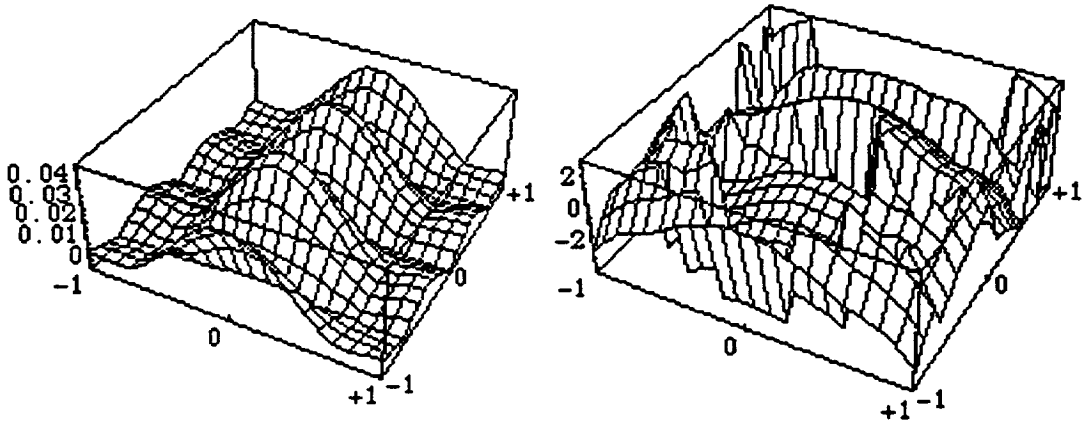

0.6 x 0.6 m aperture Max amp= 0.0451 phase

Figure 6b Amplitude & Phase L-T Term for plane wave
(@ 2 meters, λ =.19 m)

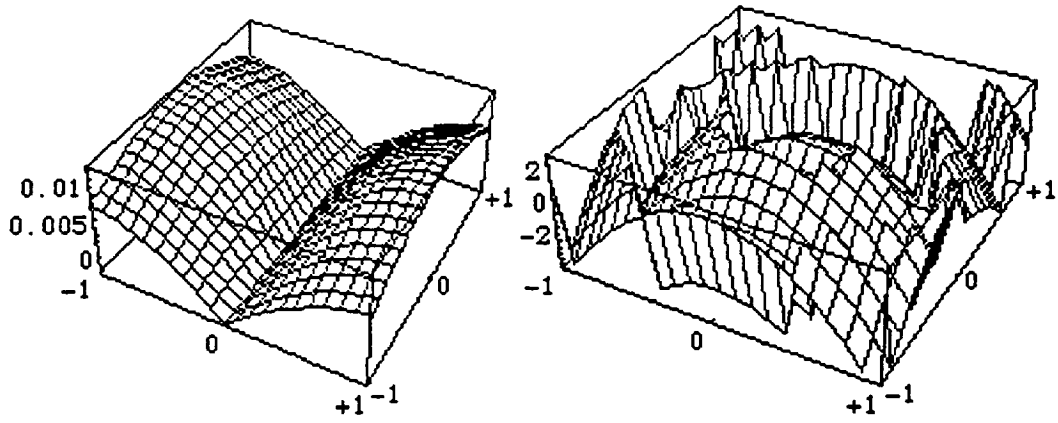

0.19 x 0.19 m aperture Max amp = 0.0133 phase

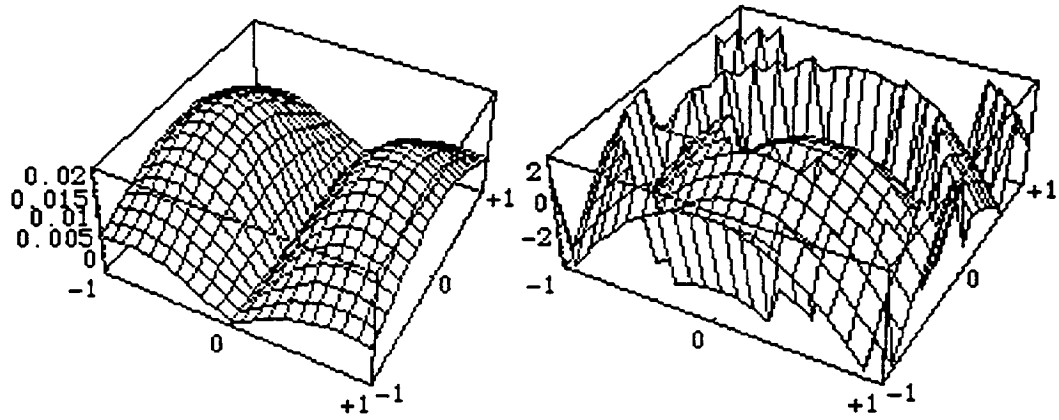

0.3 x 0.3 m aperture Max amp = 0.0225 phase

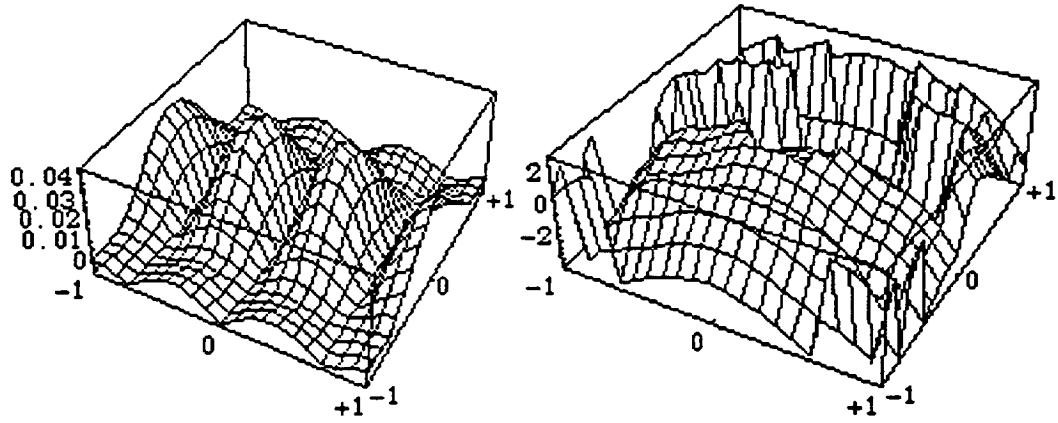

0.6 x 0.6 m aperture Max amp = 0.0452 phase

Figure 6c Amplitude & Phase Kottler Term for plane wave
(@ 2 meters, λ =.19 m)

Appendix B

Extended Kirchhoff Equations

Karczewski First Term Fresnel-Kirchhoff term Note scalar amplitude -- sum over a surface

Basic 1st term

```
ep=avec*Exp[-I*k*(qvec.pvec)] (*plane wave in*)
```

$$\text{avec}\ E^{-I\ k\ \text{qvec}\ .\ \text{pvec}}$$

```
(* p & n unit vectors  q & r not unit vectors *)
kterm1=ep*D[(Exp[-I*k*r]/r),r]*(rvec/r).nvec
```

$$\text{avec}\ E^{-I\ k\ \text{qvec}\ .\ \text{pvec}}\ \left(-\left(\frac{E^{-I\ k\ r}}{r^2}\right) - \frac{I\ E^{-I\ k\ r}\ k}{r}\right)$$

$$\left(\frac{\text{rvec}}{r}\right)\ .\ \text{nvec}$$

```
kterm2=(Exp[-I*k*r]/r)*D[ep,qvec.pvec]*pvec.nvec
```

$$\frac{-I\ \text{avec}\ E^{-I\ k\ r\ -\ I\ k\ \text{qvec}\ .\ \text{pvec}}\ k\ \text{pvec}\ .\ \text{nvec}}{r}$$

```
kterm=(1/(4*Pi))*(kterm1-kterm2)
```

$$\left(\frac{I\ \text{avec}\ E^{-I\ k\ r\ -\ I\ k\ \text{qvec}\ .\ \text{pvec}}\ k\ \text{pvec}\ .\ \text{nvec}}{r} + \text{avec}\ E^{-I\ k\ \text{qvec}\ .\ \text{pvec}}\ \left(-\left(\frac{E^{-I\ k\ r}}{r^2}\right) - \frac{I\ E^{-I\ k\ r}\ k}{r}\right)\left(\frac{\text{rvec}}{r}\right)\ .\ \text{nvec}\right) / (4\ \text{Pi})$$

```
Simplify[kterm]
```

$$\left(\frac{-I}{4}\ \text{avec}\ E^{-I\ k\ (r\ +\ \text{qvec}\ .\ \text{pvec})}\left(-(k\ r\ \text{pvec}\ .\ \text{nvec}) - I\left(\frac{\text{rvec}}{r}\right)\ .\ \text{nvec} + k\ r\left(\frac{\text{rvec}}{r}\right)\ .\ \text{nvec}\right)\right) / (\text{Pi}\ r^2)$$

□ **Put in actual values & plot**

```
k=N[2*Pi/.19]; a=b=.5; amp=1.;

xlo=-a; xhi=a;
ylo=-b; yhi=b;

avec={1,0,0};    (* input E field amp/polar vector *)
nvec={0,0,1};    (* aperture unit normal vector *)
pvec={0,0,1};      (* unit input propagation vector *)
rovec={rox,roy,2}; (* obs pt-origin vector not unit *)

qvec={eta,nu,0};  (* aperture sum vector  *)
rvec=qvec-rovec;  (* da - obs pt vector not unit *)
p=Sqrt[pvec.pvec];
r=Sqrt[rvec.rvec];
```

```
(* note kfirstterm is vector *)
kfirstterm=Simplify[N[kterm]]

(* value / graph hi-lo & del  *)
plotlo=-1 ; plothi=1; delplot=.1;
```

```
Do[
ansx=NIntegrate[Part[kfirstterm,1],
{eta,xlo,xhi},{nu,ylo,yhi},AccuracyGoal->2,
PrecisionGoal->4];

ans1[rox,roy]=N[{ansx,ansy,ansz},3];

Print[rox," ",roy," ",ans1[rox,roy]];

,{rox,plotlo,plothi,delplot},
{roy,plotlo,plothi,delplot}]
```

```
abslist=Table[Abs[First[ans1[rox,roy]]],
{rox,plotlo,plothi,delplot},
{roy,plotlo,plothi,delplot}];

Short[abslist,10]
Max[abslist]
Min[abslist]

ListPlot3D[abslist,Shading->False,
PlotRange->All,Ticks->{{{5,"-.5"},{10,"0"},{15,"+.5"}},
{{5,"-.5"},{10,"0"},{15,"+.5"}},Automatic}]
```

```
{{0.0439729, 0.0421303, 0.0488373, 0.073531, 0.100879,
   0.116565, 0.124559, 0.152015, 0.208339, 0.263591,
   0.286069, 0.263591, 0.208339, 0.152015, 0.124559,
   0.116565, 0.100879, 0.073531, 0.0488373, 0.0421303,
   0.0439729}, <<20>>}
```

```
1.76466
```

```
0.0280352
```

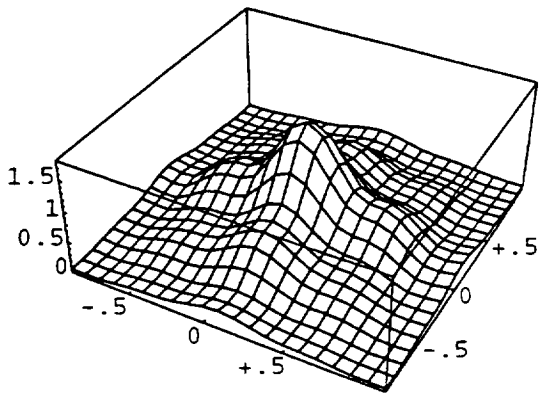


```
-SurfaceGraphics-
```

```
arglist=Table[Arg[First[ans1[rox,roy]]],
{rox,plotlo,plothi,delplot},
{roy,plotlo,plothi,delplot}];

Short[arglist,5]
Max[arglist]
Min[arglist]

ListPlot3D[arglist,Shading->False,
   Ticks->{{{5,"-.5"},{10,"0"},{15,"+.5"}},
{{5,"-.5"},{10,"0"},{15,"+.5"}},Automatic}]
```

```
{<<21>>}
```

```
2.95282
```

```
-3.07655
```

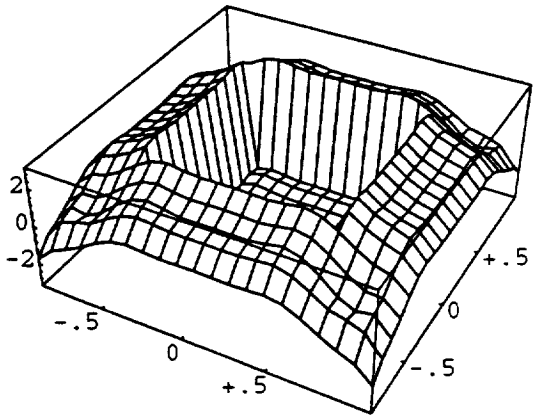

-SurfaceGraphics-

Karczewski Second Term Larmor-Tedone term Note vector amplitude -- sum over a line

basic term

```
(*input is a plane wave--amp vector is {ax,ay,az}*)
eo= {ax,ay,0}*Exp[-I*k*(qvec.pvec)]
```

$$\{ax\ E^{-I\ k\ qvec\ .\ pvec},\ ay\ E^{-I\ k\ qvec\ .\ pvec},\ 0\}$$

```
aterm={dx,dy,0}
```

$$\{dx,\ dy,\ 0\}$$

```
bterm=Simplify[eo*(Exp[-I*k*r]/r)]
```

$$\left\{\frac{ax\ E^{-I\ k\ (r\ +\ qvec\ .\ pvec)}}{r},\ \frac{ay\ E^{-I\ k\ (r\ +\ qvec\ .\ pvec)}}{r},\ 0\right\}$$

```
secondterm=Simplify[(1/(4*Pi))*CrossProduct[aterm,bterm]]
```

$$\left\{0,\ 0,\ \frac{(ay\ dx\ -\ ax\ dy)\ E^{-I\ k\ (r\ +\ qvec\ .\ pvec)}}{4\ Pi\ r}\right\}$$

Calculations & 3D plots all 4 lines (top,bottom,right,left)

```
pvec={px,py,pz};
qvec={eta,nu,0};
rovec={rox,roy,roz};
rvec=qvec-rovec;
r=Sqrt[rvec.rvec];

func2=Last[secondterm]
```

$$\frac{(ay\ dx\ -\ ax\ dy)\ Power[E,\ -I\ k\ (eta\ px\ +\ nu\ py\ +\ Sqrt[(eta\ -\ rox)^2\ +\ (nu\ -\ roy)^2\ +\ roz^2])]}{(4\ Pi\ Sqrt[(eta\ -\ rox)^2\ +\ (nu\ -\ roy)^2\ +\ roz^2])}$$

```
k=2*Pi/.19;     a=.3 ; b=.3 ;

ax=1.; ay=0.; az=0.; (*ampvec-polar@aperture*)

{px,py,pz}={0,0,1}; (* prop vector *)

{rox,roy,roz}={rox,roy,2};  (* observ pt *)

objmin=-1.; objmax=1.; objdel=.1;(*3D x image plane *)

Simplify[N[func2,3]]
```

```
(-0.0795775 2.72
      -33.1 I Sqrt[4. + (eta - 1. rox)^2 + (nu - 1. roy)^2]
     dy) / Sqrt[4. + (eta - 1. rox)^2 + (nu - 1. roy)^2]
```

□ top line

```
dx=1;  dy=0 ;
nu=b;
Do[

anstop[rox,roy]=N[NIntegrate[-func2,{eta,-a,a},
AccuracyGoal->3],3];

(*Print[rox," ",roy,"  ",Chop[anstop[rox,roy]]]; *)

,{rox,objmin,objmax,objdel},
{roy,objmin,objmax,objdel}];
```

□ bottom line

```
dx=1;  dy=0 ;
nu=-b;
Do[

ansbottom[rox,roy]=N[
    NIntegrate[func2,{eta,-a,a},AccuracyGoal->3],3];

(*Print[rox," ",roy,"  ",Chop[ansbottom[rox,roy]]];*)

,{rox,objmin,objmax,objdel},
{roy,objmin,objmax,objdel}];
```

□ **left line**

```
dx=0;  dy=1 ;
eta=a;
Do[

ansleft[rox,roy]=N[
    NIntegrate[-func2,{nu,-b,b},AccuracyGoal->3],3];

(*Print[rox," ",roy,"  ",Chop[ansleft[rox,roy]]];*)

,{rox,objmin,objmax,objdel},
{roy,objmin,objmax,objdel}];
```

□ **right line**

```
dx=0;  dy=1 ;
eta=-a;
Do[

ansright[rox,roy]=N[
    NIntegrate[func2,{nu,-b,b},AccuracyGoal->3],3];

(* Print[rox," ",roy,"  ",Chop[ansright[rox,roy]]];*)

,{rox,objmin,objmax,objdel},
{roy,objmin,objmax,objdel}];
```

□ **Sum of edges**

```
Do[
anstot[rox,roy]=anstop[rox,roy]+ansbottom[rox,roy]+
ansleft[rox,roy]+ansright[rox,roy];

(* Print[rox," ",roy,"  ",Chop[anstot[rox,roy]]];*)

,{rox,objmin,objmax,objdel},
{roy,objmin,objmax,objdel}]
```

```
Short[Table[anstot[x,y]],{x,objmin,objmax,objdel},
{y,objmin,objmax,objdel},10]
```

```
absans=Table[Abs[anstot[x,y]],{x,objmin,objmax,objdel},
{y,objmin,objmax,objdel}];
Short[absans,10]
Max[absans]
Min[absans]
```

```
ListPlot3D[absans,Shading->False,PlotRange->All,
Ticks->{{{1,"-1"},{11,"0"},{21,"+1"}},
{{1,"-1"},{11,"0"},{21,"+1"}},Automatic}]
```

```
{{0.00671825, 0.00620846, 0.00542213, 0.006125,
   0.00981294, 0.0155642, 0.0222316, 0.0288345, 0.034427,
   0.0381737, 0.0394923, 0.0381737, 0.034427, 0.0288345,
   0.0222316, 0.0155642, 0.00981294, 0.006125,
   0.00542213, 0.00620846, 0.00671825}, <<20>>}

0.0451689

0.
```

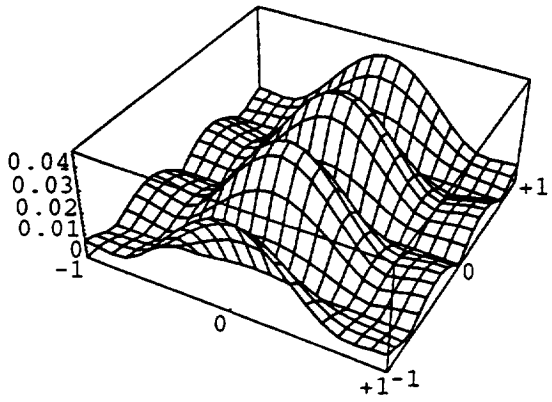


```
-SurfaceGraphics-
```

```
argans=Table[Arg[anstot[x,y]],{x,objmin,objmax,objdel},
{y,objmin,objmax,objdel}];
Short[argans,10]
Max[argans]
Min[argans]
ListPlot3D[argans,Shading->False,
Ticks->{{{1,"-1"},{11,"0"},{21,"+1"}},
{{1,"-1"},{11,"0"},{21,"+1"}},Automatic}]
```

```
{{-2.14393, -1.12203, -0.435544, -0.131995, 0.236524,
   0.747999, 1.25242, 1.67775, 1.99418, 2.18814, 2.2534,
   2.18814, 1.99418, 1.67775, 1.25242, 0.747999,
   0.236524, -0.131995, -0.435544, -1.12203, -2.14393},
  {<<21>>}, <<18>>, {0.997662, 2.01957, 2.70605, 3.0096,
   -2.90507, -2.39359, -1.88918, -1.46385, -1.14741,
   -0.95345, -0.888188, -0.95345, -1.14741, -1.46385,
   -1.88918, -2.39359, -2.90507, 3.0096, 2.70605,
   2.01957, 0.997662}}

3.10131

-3.11698
```

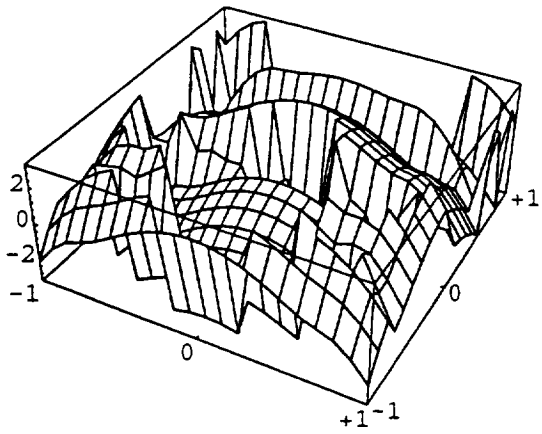

-SurfaceGraphics-

Karczewski Third term
(*run all-Note vector amplitude *)

basic term

```
eo= Exp[-I*k*(qvec.pvec)]  (* plane wave *)

dipole=Exp[-I*k*r]/r
```

$$E^{-I\ k\ qvec\ .\ pvec}$$

$$\frac{E^{-I\ k\ r}}{r}$$

```
aterm={dx,dy,0}
```

{dx, dy, 0}

```
bterm=eo*CrossProduct[pvec,avec]
```

$$E^{-I\ k\ qvec\ .\ pvec}\ CrossProduct[pvec,\ avec]$$

```
cterm=First[Grad[dipole,Spherical[r,theta,phi]]]*pvec
```

$$pvec\ \left(-\left(\frac{E^{-I\ k\ r}}{r^2}\right)\ -\ \frac{I\ E^{-I\ k\ r}\ k}{r}\right)$$

```
term3=Simplify[(1/(4*Pi*I*k)*(aterm.bterm)*cterm)]
```

$$-(E^{-I\ k\ r}\ pvec\ (-I + k\ r)\ \{dx,\ dy,\ 0\}\ .\ (E^{-I\ k\ qvec\ .\ pvec}\ CrossProduct[pvec,\ avec]))\ /\ (4\ k\ Pi\ r^2)$$

put in new values then run ---vectors for dx≠0 dy=0 y±b=±.5 *)

```
px=.; py=.; pz=.; dx=.; dy=.; eta=.;  nu=.;r=.;
ax=.;ay=.; az=.;rox=.;roy=.;roz=.;k=.;
rovec=.;avec=.;pvec=.;rvec=.;qvec=.;
```

```
func3=term3
```

$$-(E^{-I\ k\ r}\ \text{pvec}\ (-I + k\ r)\ \{dx,\ dy,\ 0\}\ .\ (E^{-I\ k\ \text{qvec}\ .\ \text{pvec}}\ \text{CrossProduct}[\text{pvec},\ \text{avec}]))\ /\ (4\ k\ \text{Pi}\ r^2)$$

```
rovec={rox,roy,roz};(*obs pt vector from origin *)
avec={ax,ay,az};  (* amp/polarization vector  *)
pvec={px,py,pz}; (* unit propagation vector *)
qvec={eta,nu,0};
rvec=qvec-rovec;  (*obs pt vector from ds *)
r=Sqrt[rvec.rvec];
```

```
k=N[2*Pi/.19,3];  a=.15 ; b=.15;

{px,py,pz}={0,0,1}; (* prop vector *)
{rox,roy,roz}={rox,roy,2};  (* observ pt *)
{ax,ay,az}={1,0,0};   (* amp-pol vector in  *)

objmin=-1 ;objmax=1;delobj=.1 ;(*image plane size*)

thirdterm=N[Simplify[func3],3]
```

$$\{0,\ 0,\ (-0.00241\ 2.72 - 33.1\ I\ \text{Sqrt}[4. + (\text{eta} - 1.\ \text{rox})^2 + (\text{nu} - 1.\ \text{roy})^2]\ dy\ (-1.\ I + 33.1\ \text{Sqrt}[4. + (\text{eta} - 1.\ \text{rox})^2 + (\text{nu} - 1.\ \text{roy})^2]))\ /\ (4. + (\text{eta} - 1.\ \text{rox})^2 + (\text{nu} - 1.\ \text{roy})^2)\}$$

```
dx=0;    dy=1;  (* ck above for proper dx or dy *)
eta=a ;

Do[

ansright[rox,roy]=NIntegrate[Last[thirdterm],
{nu,-b,b}];

(* Print[rox," ",roy,"  ",N[ansright[rox,roy],3]];*)

,{rox,objmin,objmax,delobj},{roy,objmin,objmax,delobj}]
```

```
dx=0;    dy=1;  (* ck above for proper dx or dy *)
eta=-a ;
```

```
Do[

ansleft[rox,roy]=NIntegrate[-Last[thirdterm],
{nu,-b,b}];

(*Print[rox," ",roy,"  ",N[ansleft[rox,roy],3]];*)

,{rox,objmin,objmax,delobj},{roy,objmin,objmax,delobj}]
```

```
dx=1;    dy=0;   (* ck above for proper dx or dy *)
nu=+b ;

Do[

anstop[rox,roy]=N[NIntegrate[Last[thirdterm],
{eta,-a,a}],3];

(* Print[rox," ",roy,"  ",anstop[rox,roy]]; *)

,{rox,objmin,objmax,delobj},{roy,objmin,objmax,delobj}]
```

```
dx=1;    dy=0;   (* ck above for proper dx or dy *)
nu=-b ;

Do[

ansbottom[rox,roy]=N[NIntegrate[-Last[thirdterm],
{eta,-a,a}],3];

(* Print[rox," ",roy,"  ",ansbottom[rox,roy]];  *)

,{rox,objmin,objmax,delobj},{roy,objmin,objmax,delobj}]
```

```
Do[
anstot[rox,roy]=ansright[rox,roy]+ansleft[rox,roy]+
anstop[rox,roy]+ansbottom[rox,roy];

Print[rox," ",roy,"  ",anstot[rox,roy]];

,{rox,objmin,objmax,delobj},{roy,objmin,objmax,delobj}]
```

```
absans=Table[Abs[anstot[roy,rox]],
{rox,objmin,objmax,delobj},{roy,objmin,objmax,delobj}];

Short[absans,10]
Max[absans]
Min[absans]

ListPlot3D[absans,Shading->False,PlotRange->All,
Ticks->{{{1,"-1"},{11,"0"},{21,"+1"}},
{{1,"-1"},{11,"0"},{21,"+1"}},Automatic}]
```

```
{{0.00779568, 0.00820651, 0.00836845, 0.00825102,
   0.00783507, 0.00711599, 0.00610602, 0.00483521,
   0.00335077, 0.00171473, 4.73506 10^-21, 0.00171473,
   0.00335077, 0.00483521, 0.00610602, 0.00711599,
   0.00783507, 0.00825102, 0.00836845, 0.00820651,
   0.00779568}, <<20>>}
```

```
0.0225163
```

```
0.
```

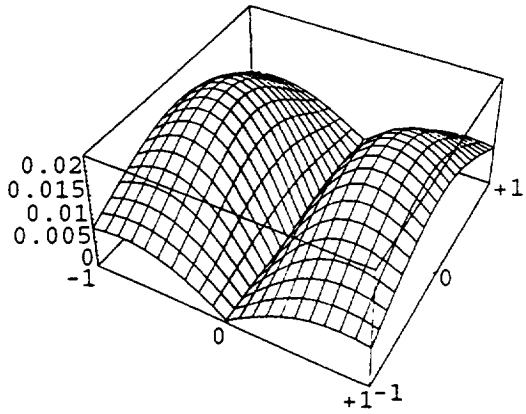


```
-SurfaceGraphics-
```

```
argans=Table[Arg[anstot[rox,roy]],
{rox,objmin,objmax,delobj},{roy,objmin,objmax,delobj}];

Short[argans,5]
Max[argans]
Min[argans]

ListPlot3D[argans,Shading->False,
Ticks->{{{1,"-1"},{11,"0"},{21,"+1"}},
{{1,"-1"},{11,"0"},{21,"+1"}},Automatic}]
```

```
{{2.11896, -2.88341, -1.71827, -0.674607, 0.242159,
   1.02709, 1.67578, 2.18445, 2.55005, 2.77033, 2.84391,
   2.77033, 2.55005, 2.18445, 1.67578, 1.02709, 0.242159,
   -0.674607, -1.71827, -2.88341, 2.11896}, <<19>>,
  {<<21>>}}

3.09887

-3.06415
```

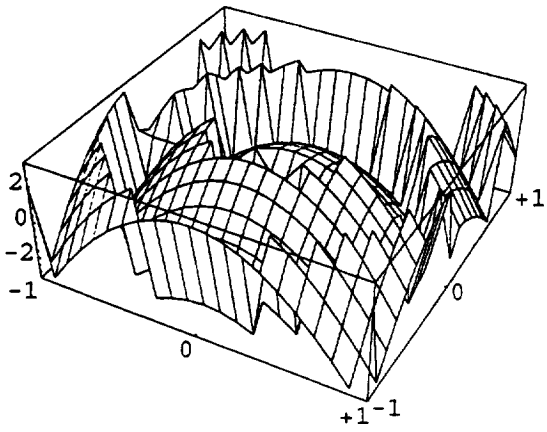


```
-SurfaceGraphics-
```

References

1Totzeck, JOSA-A Jan 1991
2 MIT Rad Lab series, Vol12, S. Silver Ed.,1948
3 Antenna Therory & Design, Stutzman & Thiele, Wiley & Sons, 1981, Figure 7-4
4 Keller, JOSA Feb 1962 or Stutzman also
5 Silver, JOSA Feb 1962
6 Contemporary Optics, Ghatak & Thyagarajan, Plenum Press, 1978
7 Born & Wolf, Sec 8.3.2
8 Jackson, Classical Electrodymanics, Sec 9.8
9 Totzeck & Krumbugel, 'Extension of Babinet's Principle & the Andrews Boundry Diffraction Wave to Weak Phase Objects', JOSA-a Dec 1994. Also see Optics, 2nd Ed., Hecht, Figure 10.78 for example.
10 Gordon, IEEE Tran on Ant. & Prop., July 1975
11Karczewski, JOSA, Oct 1961, reference to F. Kottler, Ann Physik, 1923
12 Samual Silver, JOSA, Feb 1962, page 137
13 Baker & Copson, 'The Mathematical Theory of Huygen's Principle', Oxford, 1969. See also Maggi, Annali di Mat, (2) 16 p 21-48 and Miyamoto & Wolf, 'Generalization of the Maggi-Rubinowicz Therory of the Boundary Diffraction Wave' - Part 1 & Part 2, JOSA, June 1962, page 615
14 Keller JOSA Feb 1962 reference to A Rubinowicz, Ann. Physics, 53 1917 & 73 1924
15 Baker & Copson,'The Mathematical Theory of Huygen's Principle' Clarendon Press, Oxford, 1939
16 C. J. Bouwkamp, Progress in Physics, 17, p 35-100, 1954.

REPORT DOCUMENTATION PAGE

Form Approved
OMB No. 0704-0188

1. AGENCY USE ONLY (leave blank)	2. REPORT DATE	3. REPORT TYPE AND DATES COVERED
	May 1996	Contractor Report

4. TITLE AND SUBTITLE

Multipath Analysis
Diffraction Calculations

5. FUNDING NUMBERS

C NAS1-19000
WU 478-87-00-01

6. AUTHOR(S)

Richard B. Statham

7. PERFORMING ORGANIZATION NAME(S) AND ADDRESS(ES)

Lockheed Martin Engineering & Sciences
Langley Program Office
144 Research Dr.
Hampton, VA 23666

8. PERFORMING ORGANIZATION REPORT NUMBER

LPO-SSAS-96-1

9. SPONSORING / MONITORING AGENCY NAME(S) AND ADDRESS(ES)

National Aeronautics and Space Administration
Langely Research Center
Hampton, VA 23681-0001

10. SPONSORING / MONITORING AGENCY REPORT NUMBER

NASA CR-198314

11. SUPPLEMENTARY NOTES

Langley Technical Monitor: Stephen J. Katzberg

12a. DISTRIBUTION / AVAILABILITY STATEMENT

Unclassified-Unlimited
Subject Category 19

12b. DISTRIBUTION CODE

13. ABSTRACT (Maximum 200 words)

This report describes extensions of the Kirchhoff diffraction equation to higher edge terms and discusses their suitability to model diffraction multipath effects of a small satellite structure. When receiving signals, at a satellite, from the Global Positioning System (GPS), reflected signals from the satellite structure result in multipath errors in the determination of the satellite position. Multipath error can be caused by diffraction of the reflected signals and a method of calculating this diffraction is required when using a facet model of the satellite. Several aspects of the Kirchhoff equation are discussed and numerical examples, in the near and far fields, are shown. The vector form of the extended Kirchhoff equation, by adding the Larmor-Tedone and Kottler edge terms, is given as a Mathematica model in an appendix. The Kirchhoff equation was investigated as being easily implemented and of good accuracy in the basic form, especially in phase determination. The basic Kirchhoff can be extended for higher accuracy if desired. A brief discussion of the method of moments and the geometric theory of diffraction is included, but seem to offer no clear advantage in implementation over the Kirchhoff for facet models.

14. SUBJECT TERMS

Diffraction, Kirchhoff equation, Larmor-Tedone, Kottler, Mathematica model, Maggi transform, Global Positioning System, multipath effects, microwave, satellite

15. NUMBER OF PAGES

36

16. PRICE CODE

A03

17. SECURITY CLASSIFICATION OF REPORT	18. SECURITY CLASSIFICATION OF THIS PAGE	19. SECURITY CLASSIFICATION OF ABSTRACT	20. LIMITATION OF ABSTRACT
Unclassified	Unclassified	Unclassified	UL